A Modular Three-Phase Buck-Boost Motor Drive Topology

Didem Tekgun
Dept. Of Electrical and Electronics Engineering,
Abdullah Gul University
Kayseri, Turkey
didem.tekgun@agu.edu.tr

Burak Tekgun
Dept. Of Electrical and Electronics Engineering,
Abdullah Gul University
Kayseri, Turkey
burak.tekgun@agu.edu.tr

Irfan Alan
Dept. Of Electrical and Electronics Engineering,
Abdullah Gul University
Kayseri, Turkey
irfan.alan@agu.edu.tr

***Abstract*—The voltage-source inverter (VSI) is a fundamental power electronic device to drive three-phase electrical machines with high performance. In this paper, a modular three-phase DC/Rectified AC/AC (DC/RAC/AC) inverter supplying a permanent-magnet synchronous machine (PMSM) is proposed. In this topology, the three-phase VSI is composed of three single-phase modules connected in parallel. Each single-phase inverter module consists of a non-inverting bidirectional buck-boost DC/DC converter and a cascaded H-bridge inverter. Here, the DC/DC converter generates rectified AC waveforms and the H-bridge inverter alternates these signals to create the intended AC voltage waveform. Therefore, the bulk DC Bus capacitor and boost converter inductor, which exist in a typical battery-powered voltage boosting topology can be eliminated which results in a smaller size and reduced cost. In addition, the switching losses only occur in the DC/DC converter unit and the H-bridge inverter switching losses are negligible due to the zero-voltage switching while in a conventional structure, high-frequency switching occurs both in the DC/DC converter and the six-switch inverter causing reduced overall system efficiency. The proposed inverter is controlled with a well-known field-oriented control (FOC). This paper presents the operating principle, design, and control structure of the proposed three-phase inverter. The functionality of the three-phase inverter is verified through PowerSim simulations. The proposed motor drive system is compared to the conventional one while driving a 4 kW PMSM with FOC and the whole system efficiency difference map is generated. The biggest difference is recorded as 3.8 points favoring the proposed system.**

Keywords—Three-phase modular inverter; voltage source inverter; wide bandgap devices; permanent-magnet machines; high efficiency

I. INTRODUCTION

As the world has been transforming its energy generation and consumption systems into smart, adaptive, efficient, and flexibly controllable structures, devices that are utilized in these systems need to be improved and adapted to the emerging needs. Owing to its simple structure, bidirectional power flow capability, efficiency, power density, being adaptable to the variable input-output conditions the three-phase voltage source inverter (VSI) is used extensively in all kinds of applications, such as renewable energy systems, active power filters, electric vehicles, etc. [1]–[4]. Systems that have variable input power, fluctuating input voltage makes it challenging to size the converter power electronics for both low voltage high power, and high voltage low power operating conditions. Such systems are ended up with an oversized design that is not desirable especially for high power density converters with a bulky DC bus capacitor is used in this topology to be able to filter the input current and keep the voltage level constant [5]. A large capacitor raises problems such as heat dissipation and failure protection which adds further losses and volume to the overall system.

Since the early 2000s, buck-boost DC/AC inverters attract researchers' attention due to its role in stabilization of voltage for feeding the three-phase converter with a fast-dynamic response as a low-cost solution [3], [6], [7]. To stabilize the DC bus voltage, usually, a boost converter is cascaded with a classical six-switch inverter, which is very popular especially in the renewable energy and automotive applications [8]. However, an increased number of semiconductors dealing with the high frequency and the inductive components lead to switching, core, and conductive losses as well as the size and the cost of the overall system to increase. Since the demand is to process the power with maximum efficiency with minimum size, single-stage topologies become attractive. Half-bridge series resonant buck-boost inverter [7], flyback topologies [9], [10], buck-boost DC/DC converter cascaded with unfolding full-bridge inverter [6], [11], [12], and Z-source inverter [13], [14] are mainly the single-stage inverter topologies that are used most. Some of these topologies suffer from high voltage stress, slow dynamics, some of them can process the power only in one direction, some studies can process only low power levels and some of them are stable only in a limited operating region [6]. There are three-phase topologies that use three single-phase buck-boost inverters connected to a neutral point called Y-inverters in the literature [8], [15] used as grid-connected inverters or motor drives [14], [16].

The development of the modern power semiconductor devices that increasingly improve their performance, such as Silicon Carbide (SiC) and Gallium Nitride (GaN) MOSFETs, allow higher efficiencies [17]–[19]. The VSIs that use conventional silicon devices that operate at low frequency suffer from the distorted current; therefore, power losses and inefficiency. Recent studies show the SiC MOSFETs are gaining importance in power converter designs due to their fast switching speed, ability to operate at high temperatures, with low forward voltage drop, and reduced power losses [20], [21].

Typically, a battery-powered motor drive system that requires voltage boost consists of a DC/DC boost converter to step up the battery voltage and a full-bridge inverter to drive the motor as shown in Fig.1. Such a system has bulky DC bus capacitors right before the six-switch inverter and a bulky inductor in the boost converter, which result in high cost and a large size converter. Moreover, since the high-frequency switching occurs both in the DC/DC converter unit and the six-switch inverter, high switching losses are inevitable; hence, the overall system efficiency is reduced.

In this paper, in order to satisfy the emerging needs while avoiding the aforementioned shortcomings, a special three-phase modular VSI is proposed to drive a 4-kW permanent-

978-1-7281-6264-5/20/$31.00 ©2020 IEEE

magnet synchronous machine (PMSM). In the proposed system each single-phase unit made out of a bi-directional buck-boost DC/DC converter to generate a rectified AC waveform and H-bridge inverter alternates the rectified AC waveform to generate the desired AC waveform. Hence, the DC/DC converter is the mere unit that produces the switching losses. Due to the zero-voltage switching, the switching loss of the H-bridge inverter is negligible. Furthermore, the bulk DC bus capacitor and boost converter inductor are eliminated and replaced with a small size capacitor and inductor which results in low cost and smaller size. The PMSM is controlled with a well-known field-oriented control (FOC). The aim of this work is to validate that the efficiency of the proposed system is higher than the conventional system for a wide operation range.

This paper is organized as follows: In Section II, the operating principle of the proposed inverter is introduced and discussed in detail. In Section III, a comprehensive comparison between the efficiencies of the proposed and the traditional approaches based on the actual component characteristics is conducted. The paper is concluded with a summary of the analyses in Section IV.

II. The Proposed Inverter Topology

In this section, the circuit topology and the control structure of the proposed modular three-phase inverter system is explained.

A. Circuit Topology

The proposed three-phase inverter topology utilizes three independently controlled modular single-phase inverters. Each of the single-stage has a bi-directional non-inverting buck-boost inverter and an H-bridge inverter. The non-inverting buck-boost converter consists of four high-frequency switches with anti-parallel diodes, an inductor, and a capacitor, and the unfolding H-bridge circuit has four low-frequency switches with anti-parallel diodes as shown in Fig.2.

The operating modes of the non-inverting buck-boost converter shown in Fig. 2 are given in Fig. 3.

The DC/DC converter circuit is operated in four different modes which are the combinations of motoring and generating, and buck and boost modes.

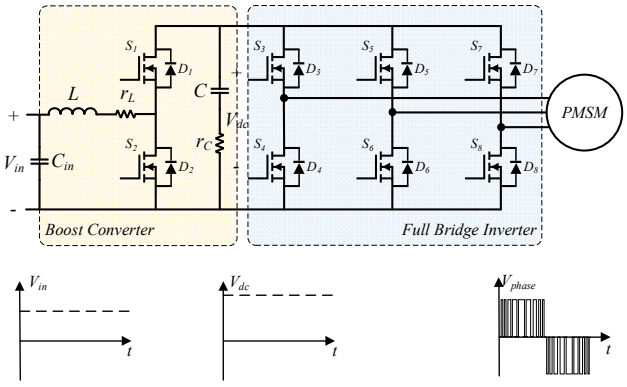

Fig. 1. The conventional voltage boosting motor drive topology and corresponding voltage waveforms.

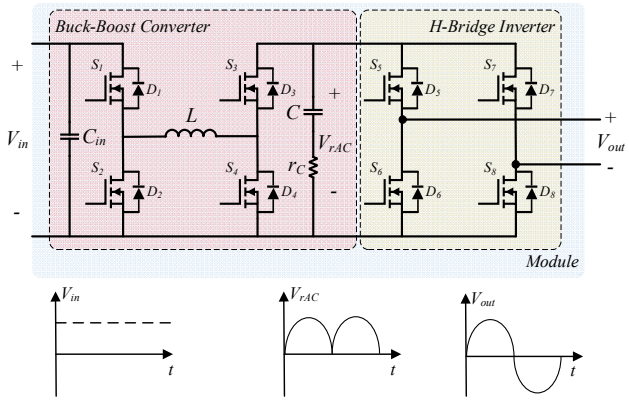

Fig. 2. Single-phase module structure containing a non-inverting buck-boost converter and an H-bridge inverter and corresponding voltage waveforms.

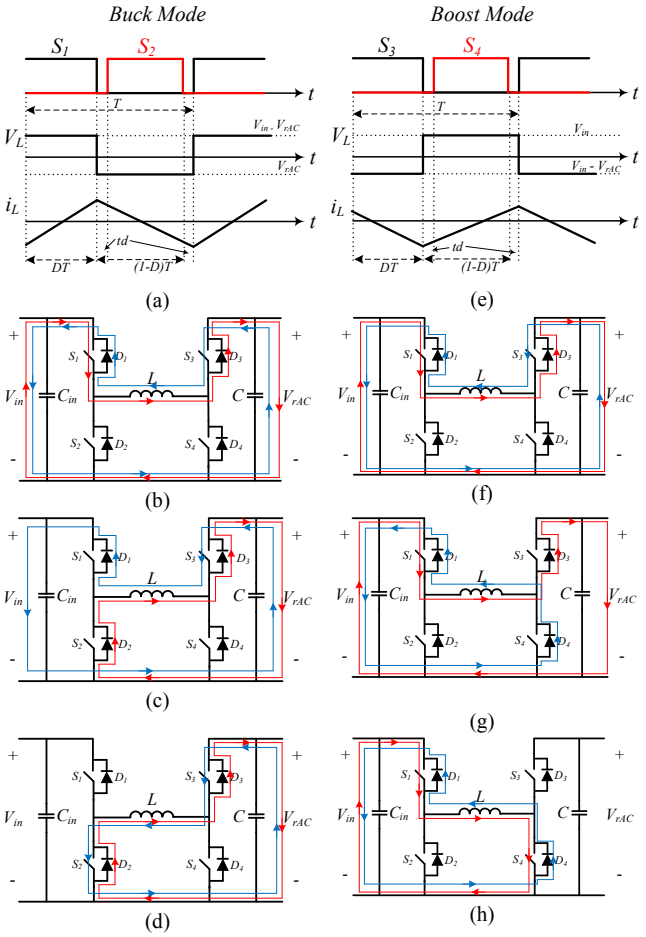

Fig. 3. In motoring mode (red lines), buck operation: (a) the switching pattern, inductor voltage, and inductor current, and the circuit modes when (b) $0 < t < DT$, (c) $DT < t < DT+td$, *and* (d) $DT+td < t < T$; boost operation: (e) the switching pattern, inductor voltage, and inductor current, and the circuit modes when (f) $0 < t < DT$, (g) $DT < t < DT+td$, *and* (h) $DT+td < t < T$.

In motoring mode (red lines in Fig.3), when the buck-boost converter operates in buck mode, the S_3 switch is fully turned on and S_4 is fully turned off, while S_1 and S_2 switches alternately operate to form a synchronous buck converter. The switching pattern, inductor voltage and current are given in Fig. 3.a. During this operation the circuit modes at the time intervals of $0 < t < DT$, $DT < t < DT+t_d$, *and* $DT+t_d < t < T$ are presented in Figs. 3.b, 3.c, and 3.d, respectively.

While operating in motoring mode when the circuit working as a boost converter the S_1 switch is fully turned on, S_2 is fully turned off, and the S_3 and S_4 switches alternate to

form a synchronous boost converter. The switching pattern, inductor voltage and current are given in Fig. 3.e. During this operation the circuit modes at the time intervals of $0 < t < DT$, $DT < t < DT+t_d$, and $DT+t_d < t < T$ are shown in Figs. 3.f, 3.g, and 3.h, respectively.

The synchronous control of the alternating switches has the advantage of eliminating the high power loss in the diodes; hence, both buck and boost modes are controlled synchronously.

The generating mode also has the buck and boost operating modes. Since the non-inverting buck-boost converter has a symmetrical structure, the control will be the same but the current directions will be flipped. Therefore, a further explanation for the generating case will not be presented in this paper.

The proposed three-phase system that is formed with three single-phase modules is shown in Fig. 4.

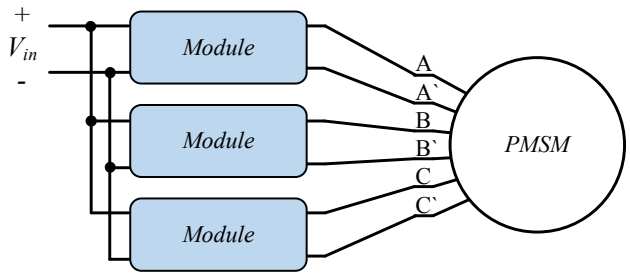

Fig. 4. Three-phase system connection diagram.

In the conventional voltage boosting motor drive system, the input voltage is boosted to a higher and more stable level to be able to generate the required current levels in the windings as illustrated in Fig. 1. Then the six-switch inverter generates a pulsating voltage waveform that has the maximum average value of 58% of the DC bus voltage, which in case the modulation is selected as space vector modulation (SVM) for smooth and silent operation. In such a system, the high-frequency switching is presented in both DC/DC conversion and DC/AC inversion stages. Additionally, the inductor used in the boost converter and the DC bus capacitor bank are bulky and lossy, which make them cost-ineffective, efficiency and reliability deteriorating factors. On the other hand, in the proposed topology switching losses only occur at the DC/DC conversion as the H-bridge converter switches when the voltage is zero while the high frequency switching capability of the wide bandgap devices helps to reduce the filter inductor and capacitor sizes. Consequently, the switching losses are reduced, bulk capacitor and inductor are replaced with smaller ones, and total system efficiency and the reliability of the system are improved.

B. Control Method

The FOC is one of the vector-based closed-loop methods that has been widely used in the motor drive industry since it allows one to control the speed of a PMSM with fast dynamic response and high efficiency [22]. Torque and speed can be independently controlled by using the FOC where two currents; *q* axis and *d* axis current; responsible for the torque and the field generation are separately resolved and controlled by current regulators, which are usually the PI controllers. The resulting *d-q* voltages are transformed back to the three-phase voltages and finally, these voltages are fed to the space vector modulator to generate the required PWM pulses to drive the inverter. A basic form of this control technique is illustrated in Fig. 5, where only the FOC current regulation portion is shown. Cascaded controllers are needed for speed and position control to adjust the d-q current references. In this study, only the torque control structure that is used in a variety of industrial and automotive traction applications is considered; hence, it is sufficient to highlight the advantages of the proposed topology.

The units replaced by the proposed inverter is shown in Fig. 6. In the conventional topology, the voltage generation system uses an open-loop control structure, i.e. there is not any voltage feedback to correct the voltage errors raised by the inverter non-idealities.

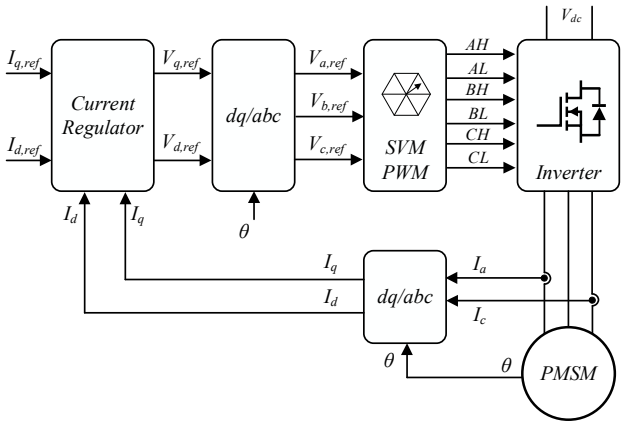

Fig. 5. Basic PMSM FOC diagram.

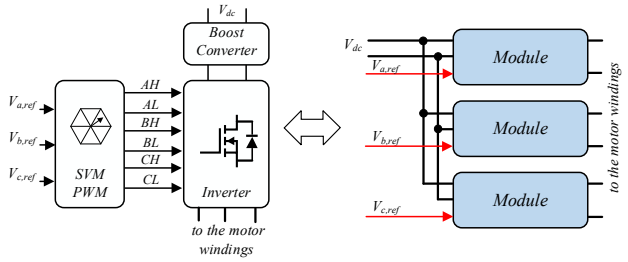

Fig. 6. The unit that replaced by the proposed inverter in the PMSM FOC.

Similarly, the proposed buck-boost inverter adopts the open-loop structure while generating the duty cycles. The reference voltage is first compared with zero to decide whether positive or negative alternance is generated and switches S_5, S_6, S_7, and S_8 are triggered accordingly. Then the reference signal is rectified and normalized based on the input voltage. This normalized input voltage defines the conversion ratio of the converter. After limiting this signal between zero and one, the switches S_1 and S_2 are controlled with it. For controlling the switches S_3 and S_4, the normalized input reference voltage is passed through a one-dimensional lookup table (LUT) to linearize the boost converter operation. The control system block diagram is presented in Fig. 7, the variation of the duty ratios when the reference varies between zero and three is shown in Fig. 8. The conversion ratio is limited to 3 for stable and safe operation.

This simple and straightforward control structure allows the power to flow in either direction as this feature is required to drive an AC motor considering the power factor may not

be unity at all times and power may be flowing from the machine to the source.

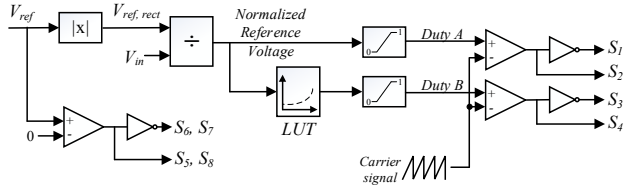

Fig. 7. The open-loop voltage control structure of the proposed buck-boost inverter.

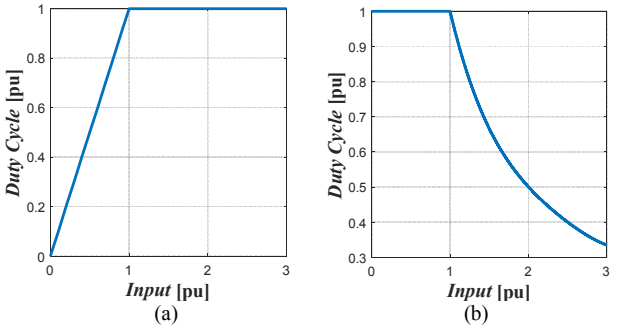

Fig. 8. (a) Duty cycle of the S_1 (S_2 alternates) switch vs. the normalized input voltage reference; (b) duty cycle of the S_3 (S_4 alternates) switch vs. the normalized input voltage reference.

III. Performance Evaluation

A. Simulations

A set of simulations are performed to validate the proposed system's superiority. A 4-kW motor drive system is simulated with both conventional and proposed systems using FOC at the constant speed constant torque conditions. A coupled dynamometer system rotates the machine at the rated speed, and the current regulators control the field and the torque currents to generate various powers on the motor shaft. The machine used in this example is a 4-kW non-salient PMSM (surface-mounted permanent magnets) with incremental encoder feedback and its specifications are given in Table I.

TABLE I. PMSM Specifications

Parameter	Value
Type	Surface-mounted PMS
Rated Power	4 kW
Rated Speed	3000 rpm
Rated Current	12.5 Arms
Rated Torque	12.5 Nm
Rated Voltage	400 Vdc
Number of Poles	8
Winding Self Inductance	2.2 mH
Winding Resistance	0.8 Ω

The conventional system and the proposed system both systems use CREE`s C3M0065090J SiC MOSFETs and have 100 V input voltage. The conventional system boosts the voltage up to 400 V first and drives the machine with the six-switch inverter. The proposed system generates the required voltage waveform for each phase during the DC/DC conversion stage and alternates it with the H bridge inverter.

The simulations are done in PowerSim platform with the parameters presented in Table II. Here, the database model feature of the PowerSim software is used to estimate the SiC device losses [23]. This feature simulates the switching behavior of the device accurately using the electrical characteristics like V_{DS} vs. I_{DS}, E_{ON}, E_{OFF} vs. R_g, etc. from the device datasheet.

B. Results

In the case study, the I_d current is kept zero for the entire simulation period, the I_q current was zero and set to 17.7 A (12.5Arms) at t = 10 msec. The reference current I_q, actual I_q, and I_d waveforms are presented in Fig. 9, which shows the current regulation works properly. After the *dq* to *abc* transformation and the SVM, reference phase voltage, generated phase voltages on both systems, and line-to-line voltage waveforms are presented in Fig. 10. Here, the V_{aref} is the reference phase voltage to be generated, V_{a1} is the filtered phase voltage waveform of the conventional system, V_{a2} is the generated phase voltage waveform with the proposed system, and V_{AB} is the line to line voltage. It can be noted that the V_{a2} waveform has some high-frequency harmonics and looks distorted due to the DC/DC converter harmonics. However, it should be kept in mind that V_{a2} is the voltage waveform directly applied to the machine while V_{a1} is the filtered 20 kHz pulsed voltage waveform at the output of the six-switch inverter.

TABLE II. Simulation Parameters

		Parameter	Value
Conventional Voltage Boosting Drive Topology	Boost Converter	Input voltage	100 V
		Output voltage	400 V
		Inductor	0.5 mH
		Inductor resistance	40 mΩ
		Output capacitor	1 mF
		Output capacitor series resistance	47 mΩ
		Switching frequency	20 kHz
		Switching device	Cree C3M0065090J
		Gate resistance	8.2 Ω
		Input voltage	400 V
	Six-Switch Inverter	Modulation	Space Vector Modulation
		Switching frequency	20 kHz
		Switching device	Cree C3M0065090J
		Gate resistance	8.2 Ω
Proposed Modular Bidirectional Buck-Boost Inverter		Input voltage	100 V
		Inductor	100 µH
		Inductor resistance	1 mΩ
		Output Capacitor	10 µF
		Output capacitor series resistance	12 mΩ
		Switching device	Cree C3M0065090J
		Gate resistance	8.2 Ω
		Switching frequency	100 kHz

The phase-A currents are presented in Fig. 11 where I_{a1} and I_{a2} are the phase currents of the conventional and the proposed systems. The output torque transients during the operation are shown in Fig. 12. These set of voltage, current, and torque waveforms validates that all the simulations are done under the same conditions.

Table III shows the efficiencies of each subsystem at 3000 rpm speed while generating 12.5 Nm and 6.25 Nm torque on the shaft.

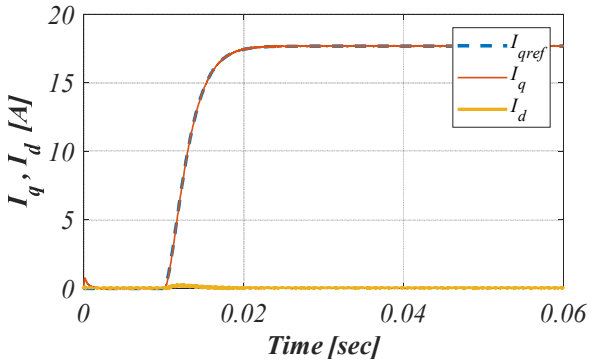

Fig. 9. Field and torque currents for both conventional and proposed systems.

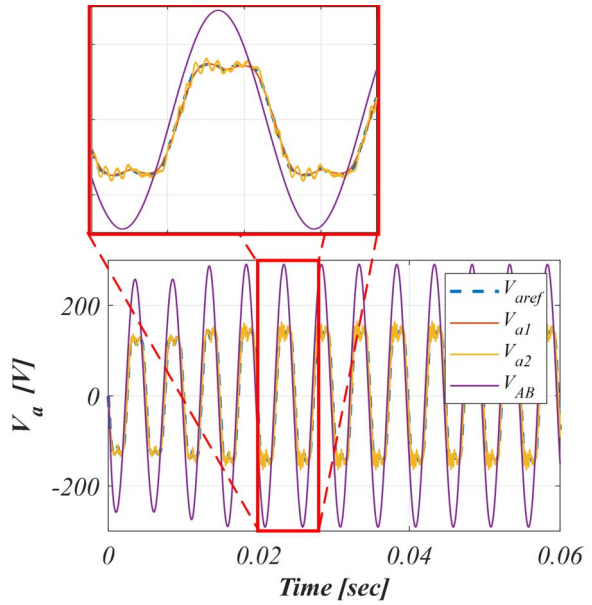

Figure 10. Phase and line lo line voltage waveforms.

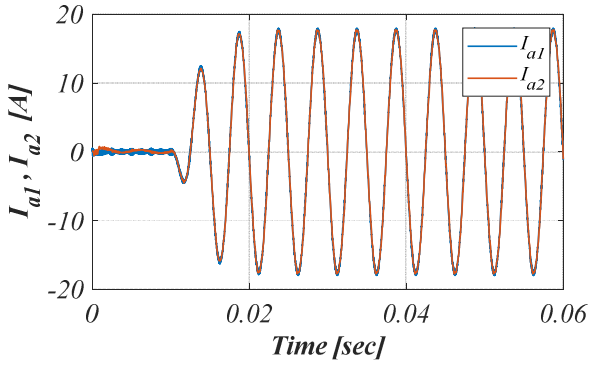

Figure 11. Phase-A current waveforms.

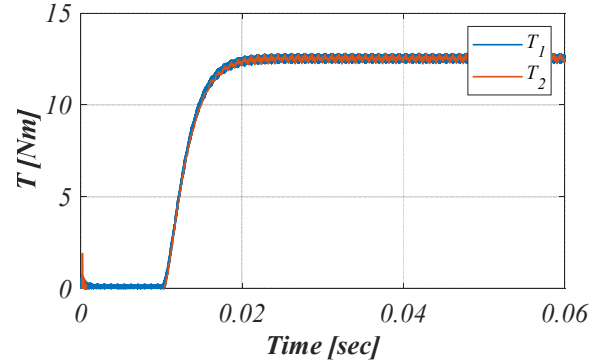

Figure 12. Resulting torque outputs on the shaft.

For the given operating conditions the difference of the total efficiency is observed as varying 3.80 and 1.64 points favoring the proposed system. Similarly, the simulations are repeated for various operating conditions to generate an efficiency difference map as presented in Fig. 13. This map clearly highlights the advantage of the proposed topology in terms of total system efficiency.

TABLE III. PERFORMANCE COMPARISON AT 3000 RPM

	Output Torque	12.5 Nm	6.25 Nm
	Output Power	4 kW	2 kW
Conventional	Boost converter efficiency	92.45%	96.25%
	Inverter efficiency	99.33%	99.65%
	Motor efficiency	91.14%	95.20%
	Total efficiency	83.69%	91.30%
Proposed	Modules efficiency	96.04%	98.12%
	Motor efficiency	91.09%	94.72%
	Total efficiency	87.48%	92.94%
	Difference (points)	3.80	1.64

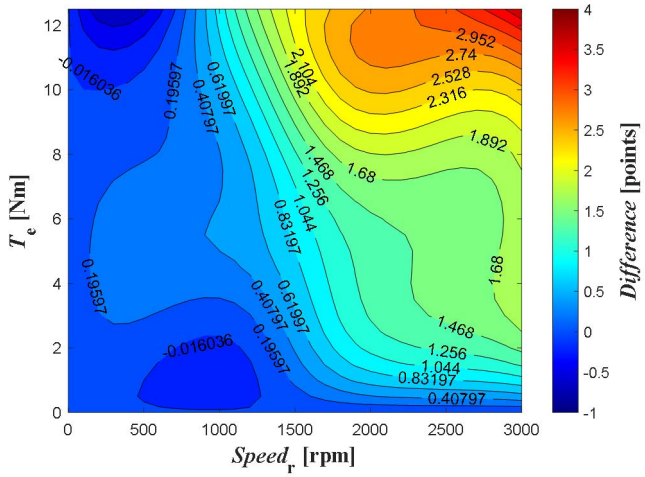

Fig. 13. Efficiency improvement map.

IV. CONCLUSIONS

This paper presents a comprehensive comparison study between the conventional voltage boosting three-phase motor drive topology and the proposed modular DC/Rectified AC/AC drive topology while driving a 4-kW non-salient permanent magnet synchronous machine (PMSM). A typical voltage boosting motor drive system usually employs a boost converter and a three-phase inverter to generate the required voltage waveforms. The proposed system contains three single-phase modules, each one of them has a buck-boost converter and an H-bridge inverter. In the conventional topology, the switching loss occurs at both units as both of them operate at high frequency. Additionally, this system requires a bulky inductor and a capacitor which adds more losses, increases the size, and affects the reliability. On the other hand, the proposed system generates the required voltage waveform's rectified version in the DC/DC conversion stage and alternates this waveform with an H-bridge inverter. Hence, the switching loss only occurs at the DC/DC converter unit. Also, this topology uses wide bandgap devices that allow high-frequency operation and consequently reducing the filter component sizes.

In the simulations, both topologies are used as a motor drive system to control a 4-kW PMSM using field-oriented control (FOC) technique. An efficiency difference map for the entire system is generated for various torque-speed operations points. It is observed that the proposed system operated at higher system efficiency almost all the operating points and the highest efficiency difference is recorded as 3.8 points favoring the proposed system.

ACKNOWLEDGMENT

This research is supported by The Scientific and Technological Research Council of Turkey (TUBITAK) under Grant 118E172.

REFERENCES

[1] M. Yilmaz and P. T. Krein, "Review of battery charger topologies, charging power levels, and infrastructure for plug-in electric and hybrid vehicles," IEEE Trans. Power Electron., vol. 28, no. 5, pp. 2151–2169, 2013.

[2] Xiong Liu, Peng Wang, and Poh Chiang Loh, "A Hybrid AC/DC Microgrid and Its Coordination Control," IEEE Trans. Smart Grid, vol. 2, no. 2, pp. 278–286, Jun. 2011.

[3] D. Voglitsis, N. Papanikolaou, and A. C. Kyritsis, "Incorporation of Harmonic Injection in an Interleaved Flyback Inverter for the Implementation of an Active Anti-Islanding Technique," IEEE Trans. Power Electron., vol. 32, no. 11, pp. 8526–8543, 2017.

[4] A. R. Boynuegri, "A power management unit with a polarity changing inverter for fuel cell/ultra-capacitor hybrid power systems," Int. J. Hydrogen Energy, vol. 42, no. 43, pp. 26924–26932, 2017.

[5] H. Ye, Y. Yang, and A. Emadi, "Traction inverters in hybrid electric vehicles," 2012 IEEE Transp. Electrif. Conf. Expo, ITEC 2012, pp. 2–7, 2012.

[6] Ankit, S. K. Sahoo, S. Sukchai, and F. F. Yanine, "Review and comparative study of single-stage inverters for a PV system," Renew. Sustain. Energy Rev., vol. 91, no. March 2017, pp. 962–986, 2018.

[7] Chien-Ming Wang and Teng-Jen Chen, "Novel single-stage half-bridge series-resonant buck-boost inverter," IEEE Trans. Aerosp. Electron. Syst., vol. 40, no. 4, pp. 1262–1270, Oct. 2004.

[8] M. Antivachis, D. Bortis, L. Schrittwieser, and J. W. Kolar, "Three-phase buck-boost Y-inverter with wide DC input voltage range," Conf. Proc. - IEEE Appl. Power Electron. Conf. Expo. - APEC, vol. 2018-March, pp. 1492–1499, 2018.

[9] H. Kim, J. S. Lee, and M. Kim, "Downsampled Iterative Learning Controller for Flyback CCM Inverter," IEEE Trans. Ind. Electron., vol. 65, no. 1, pp. 510–520, Jan. 2018.

[10] Y. Li and R. Oruganti, "A low cost flyback CCM inverter for AC module application," IEEE Trans. Power Electron., vol. 27, no. 3, pp. 1295–1303, 2012.

[11] M. Çelebi and I. Alan, "A novel approach for a sinusoidal output inverter," Electr. Eng., vol. 92, no. 7–8, pp. 239–244, 2010.

[12] F. Tian, H. Al-Atrash, R. Kersten, C. Scholl, K. Siri, and I. Batarseh, "A single-staged PV array-based high-frequency link inverter design with grid connection," Conf. Proc. - IEEE Appl. Power Electron. Conf. Expo. - APEC, vol. 2006, pp. 1451–1454, 2006.

[13] Fang Zheng Peng, "Z-source inverter," IEEE Trans. Ind. Appl., vol. 39, no. 2, pp. 504–510, Mar. 2003.

[14] R. Adle, M. Renge, S. Muley, and P. Shobhane, "Photovoltaic Based Series Z-source Inverter fed Induction Motor Drive with Improved Shoot through Technique," Energy Procedia, vol. 117, pp. 329–335, 2017.

[15] A. Darwish, A. M. Massoud, D. Holliday, S. Ahmed, and B. W. Williams, "Single-Stage Three-Phase Differential-Mode Buck-Boost Inverters with Continuous Input Current for PV Applications," IEEE Trans. Power Electron., vol. 31, no. 12, pp. 8218–8236, 2016.

[16] F. Karbakhsh, M. Amiri, and H. Abootorabi Zarchi, "Two-switch flyback inverter employing a current sensorless MPPT and scalar control for low cost solar powered pumps," IET Renew. Power Gener., vol. 11, no. 5, pp. 669–677, 2017.

[17] M. Zdanowski, D. Peftitsis, S. Piasecki, and J. Rabkowski, "On the Design Process of a 6-kVA Quasi-Z-inverter Employing SiC Power Devices," IEEE Trans. Power Electron., vol. 31, no. 11, pp. 7499–7508, 2016.

[18] F. Shang, A. P. Arribas, and M. Krishnamurthy, "A comprehensive evaluation of sic devices in traction applications," 2014 IEEE Transp. Electrif. Conf. Expo Components, Syst. Power Electron. - From Technol. to Bus. Public Policy, ITEC 2014, 2014.

[19] S. Jahdi, O. Alatise, C. Fisher, Li Ran, and P. Mawby, "An Evaluation of Silicon Carbide Unipolar Technologies for Electric Vehicle Drive-Trains," IEEE J. Emerg. Sel. Top. Power Electron., vol. 2, no. 3, pp. 517–528, 2014.

[20] M. Holz, G. Hultsch, T. Scherg, and R. Rupp, "Reliability considerations for recent Infineon SiC diode releases," Microelectron. Reliab., vol. 47, no. 9-11 SPEC. ISS., pp. 1741–1745, 2007.

[21] A. Agarwal et al., "600 V , 1- 40 A , Schottky Diodes in SiC and Their Applications," Cree White Pap., no. 919, 2010.

[22] Leon, J.I., "High-Performance Motor Drives," in Industrial Electronics Magazine, IEEE , vol.5, no.3, pp.6-26, Sept. 2011.H. Simpson, Dumb Robots, 3rd ed., Springfield: UOS Press, 2004, pp.6-9.

[23] PSIM, "Loss Calculation and Transient Analysis of SiC and GaN Devices," July 2018.